The Canadian Mineralogist
Vol. 40, pp. 419-433 (2002)

AN UNUSUAL OCCURRENCE OF Pd, Pt, Au, Ag AND Hg MINERALS IN THE PILBARA REGION OF WESTERN AUSTRALIA

ERNEST H. NICKEL§

Exploration & Mining, CSIRO, Private Bag no. 5, PO Wembley, W.A., 6913, Australia

ABSTRACT

A small high-grade occurrence of palladium, platinum, gold, silver, selenium and mercury at Copper Hills in the East Pilbara region of Western Australia exhibits a remarkable diversity of minerals and textures. Most of the mineralization occurs within a malachite–quartz host, with particularly high concentrations in malachite nodules. The primary minerals include a number of selenides, including oosterboschite, naumannite, chrisstanleyite, berzelianite, umangite, luberoite (?) and tiemannite, as well as some unidentified minerals. Other ore minerals include native gold, native silver and potarite. Oxidation of the Pd and Pt selenides has produced a range of fine-grained oxide mixtures. The Pd and Pt selenides and their oxidized products occur as fine-grained dispersions, commonly as arborescent fronds, and as larger inclusions in the malachite nodules. The native silver has been partially replaced by bromian chlorargyrite. The source of the mineralization is believed to have been acid, saline hydrothermal solutions charged with the precious metals, mercury, selenium and copper. Interaction of these solutions with dolomitic carbonate probably caused the precipitation of the minerals of economic interest.

Keywords: malachite, oosterboschite, naumannite, chrisstanleyite, berzelianite, umangite, gold, silver, platinum, palladium, Copper Hills, East Pilbara, Australia.

SOMMAIRE

Un petit indice à teneur élevée en palladium, platine, or, argent, sélénium et mercure à Copper Hills, dans le secteur oriental de la région de Pilbara, en Australie occidentale, fait preuve d'une diversité remarquable de minéraux et de textures. La zone minéralisée se trouve surtout dans un hôte de malachite + quartz contenant une concentration de nodules de malachite. Parmi les minéraux primaires se trouvent plusieurs séléniures, y inclus oosterboschite, naumannite, chrisstanleyite, berzélianite, umangite, lubéroïte (?) et tiémannite, de même que quelques minéraux non identifiés. Parmi les autres minéraux d'intérêt économique se trouvent or natif, argent natif et potarite. L'oxydation des séléniures de Pd et de Pt a produit une série de mélanges d'oxydes à granulométrie fine. Les séléniures de Pd et de Pt et les produits de leur oxydation forment des traînées à grains fins, généralement sous forme de frondes arborescentes, aussi bien que des inclusions dans les nodules de malachite. L'argent natif a partiellement été remplacé par la chlorargyrite bromifère. La source de la minéralisation serait une saumure hydrothermale acide portant métaux précieux, mercure, sélénium et cuivre. L'interaction de telles solutions avec un carbonate porteur de dolomite aurait causé la précipitation des minéraux d'intérêt économique.

(Traduit par la Rédaction)

Mots-clés: malachite, oosterboschite, naumannite, chrisstanleyite, berzélianite, umangite, or, argent, platine, palladium, Copper Hills, East Pilbara, Australie.

INTRODUCTION

The assemblage described herein is from the Copper Hills occurrence (Lat. 22°55', Long. 123°13'), at the edge of the Great Sandy Desert, in the East Pilbara region of Western Australia. It is designated as the PM location on the Blanche–Cronin 1:100,000 Geological Series map sheet of the Geological Survey of Western Australia. The occurrence is within the Tabletop Terrane of the Rudall Complex, which consists of early Proterozoic schist, amphibolite and metasedimentary rocks of lower amphibolite facies (Hickman & Bagas 1995, Bagas 1999). The Copper Hills occurrence is a small vein-type polymetallic deposit (of the order of 100 tonnes) dominated by malachite and containing native gold and silver, selenides of palladium, platinum, copper, silver and mercury, and oxides of palladium and platinum. Although samples collected during the early

§ *E-mail address*: e.nickel@per.dem.csiro.au

exploration phase contained remarkably high Pd, Pt, Au and Ag values, subsequent intensive exploration efforts have failed to reveal sufficient quantities of this material to warrant mining operations.

The mineralogical features described in this paper were obtained from the examination of some 29 polished sections produced from five hand specimens provided by geologists from the companies controlling the deposit, originally Prosilver Nominees Pty Ltd. and, later, Australian Platinum Mines NL. The specimens are reported to be typical of the high-grade portion of the occurrence, according to geologists responsible for the project. Much of the original material has been destroyed as a result of assay and analytical procedures and metallurgical testing, and therefore a complete mineralogical description of the occurrence can never be made. However, I believe that the minerals in the assemblage, and their textures, are of sufficient general interest to warrant publication.

A mineralogical investigation of the assemblage was initiated by Jiri Just, consulting mineralogist. After Mr. Just's premature death in 1994, I continued the investigation on the basis of specimens left by Mr. Just and on additional material provided by the exploration companies. A preliminary report on the occurrence was presented at the 17th General Meeting of the International Mineralogical Association (Nickel 1998).

Specimens of the material are preserved in the mineral collection of Exploration & Mining, CSIRO, and a specimen has been donated to the Museum of Victoria, Melbourne, Australia.

Mineralogical Description

The material available for study consisted of five hand-sized specimens of rock containing mineralized pods of a green to black mineral assemblage, up to about 60 mm across, in a pale brown dolomite-rich carbonate assemblage. The pods exhibit irregular and contorted banding. In general, the banding consists of a fine-grained relatively homogeneous layer and a complex layer displaying a botryoidal texture (Fig. 1). The fine-grained layer consists largely of an intimate intergrowth of malachite, quartz and goethite, whereas the complex layer is composed of a heterogeneous assemblage of dark nodules, nodular fragments and arborescent masses in a malachite–quartz matrix (Figs. 2–4). These features will be discussed in greater detail below.

Malachite, $Cu_2CO_3(OH)_2$

The dominant mineral in the mineralized pods is malachite, of which three main types can be discerned: a bright green unmineralized malachite, a "ferruginous malachite" consisting of a fine-grained greyish green intergrowth with quartz and goethite, and mineralized material that consists mainly of nodular malachite with abundant inclusions of opaque minerals.

The unmineralized malachite is fine-grained and generally contains finely intergrown quartz and occasional chrysocolla. These minerals form the matrix for the nodules of mineralized malachite and also occur as irregular masses within the mineralized malachite.

The ferruginous malachite consists of a fine-grained intergrowth of malachite, quartz and goethite, and hosts sporadic concentrations of finely disseminated particles of copper selenides and occasional gold grains. This material forms the greyish green band shown at the bottom of Figure 1.

The mineralized malachite is usually black owing to fine-grained dispersions of opaque particles. In oil immersion in transmitted light, it is opaque except at thin edges of grains, where individual micrometric inclusions can be seen. The mineralized malachite occurs in a wide variety of forms, including nodules and nodular fragments (Figs. 2, 3, 4, 5), arborescent fronds (Fig. 4), balloon-like formations (Fig. 6), and irregular grains (Fig. 7).

The finely dispersed particles in the mineralized malachite occur as concentric zones in efflorescent nodules (Fig. 8) and as "clouds" of arborescent fronds (Fig. 9). As will be shown later, these finely dispersed particles are probably luberoite, but it has not been possible to confirm their identity.

In addition to the fine-grained dispersions of luberoite (?), some of the mineralized malachite contains larger grains, mainly of palladium oxides, the distribution of which tends to conform to the external morphology of the spherical nodules (Fig. 5). Pd oxides also occur as thin concentric layers or crescents in the malachite (Fig. 8).

Berzelianite, Cu_2Se and umangite, Cu_3Se_2

Berzelianite and umangite occur as local concentrations of finely disseminated grains in the ferruginous malachite; individual grains of berzelianite are generally less than 20 μm in diameter, whereas those of umangite are slightly larger. Berzelianite is isotropic and bluish white in reflected light; umangite is pink and highly anisotropic.

An electron-microprobe analysis of umangite (Table 1) shows that it contains an appreciable amount of Pt, Ag, Hg and Pd. The standard deviations, particularly that associated with Ag, are substantial, which indicates that the minor elements are probably due to submicroscopic inclusions of extraneous minerals; this could also be expected from crystallochemical considerations, as the ionic radii of these elements are much greater than that of Cu and would therefore not readily substitute for this element in the umangite structure. The 2% S shown in the analysis could reasonably be expected to substitute for Se.

Naumannite, Ag_2Se

Naumannite occurs as grains up to 2 mm in diameter comprising the core of some of the malachite nodules. The mineral is yellowish grey and weakly anisotropic in reflected light. An electron-microprobe analysis (Table 1) gave a composition reasonably close to theoretical Ag_2Se; the high standard deviations for the minor elements Cu, Pt and Hg cast doubt on their incorporation in the structure. Minor amounts of naumannite were also observed as inclusions in native silver and as a core of grains rimmed by tiemannite (HgSe).

The large grains of naumannite have a corroded appearance (Fig. 10), and are enclosed by chalcomenite, a product of the oxidation of naumannite.

Chrisstanleyite, $Ag_2Pd_3Se_4$ and its Cu-dominant analogue

Chrisstanleyite is a relatively new mineral species, described for the first time by Paar *et al.* (1998). In the Copper Hills assemblage, the mineral is copper-bearing, and occurs as an intergrowth with its Cu-dominant analogue, possibly a new mineral (Roberts *et al.*, in prep.). Compositions determined by electron microprobe (49 spot analyses of eight grains) vary in Ag/(Ag + Cu) value from 0.02 to 0.87, with the two extreme compositions shown in Table 2. This compositional variation suggests that $Ag_2Pd_3Se_4$ and $Cu_2Pd_3Se_4$ form a solid-solution series, a suggestion supported by the observation that the two phases are indistinguishable in reflected light. They are yellow in reflected light with weak bireflectance and moderate anisotropy. They tend to be closely associated with naumannite, in which they occur as inclusions. In one polished section, they occur as a crescent of grains in naumannite and the selenate mineral, chalcomenite (Fig. 10), which suggests that chrisstanleyite and its copper-rich equivalent probably existed as a depositional layer in naumannite, and that oxidation of the selenides to a selenate has proceeded along the boundary between the two.

Oosterboschite, $(Pd,Cu)_7Se_5$ and the product of its alteration

Oosterboschite was identified primarily on the basis of its chemical composition (Table 3), which gives the empirical chemical formula $Pd_{3.9}Cu_{2.6}Se_{5.5}$, simplified to $Pd_4Cu_3Se_5$. The fact that the analytical total exceeds 100%, and that the empirical composition departs appreciably from that of the type-locality oosterboschite, $(Pd,Cu)_7Se_5$ (Johan *et al.* 1970), can probably be attributed to the lack of suitable electron-microprobe standards. Confirmation of oosterboschite by X-ray-diffraction analysis was not possible because of the small grain-size and dispersed nature of the mineral. However, its appearance in reflected light, *i.e.*, yellow color, weak bireflectance and moderate anisotropy, conforms to the original description of oosterboschite.

Oosterboschite was seen only in nodules of mineralized malachite, where it occurs as irregular grains (Fig. 11) and veinlets (Fig. 12). The larger grains are usually rimmed by a darker phase (Fig. 11), apparently a product of the decomposition of oosterboschite. At moderate magnification, the alteration product is grey in contrast to the oosterboschite, and seems to be homogeneous, but at high magnification (Fig. 11), it is seen to be an extremely fine-grained mixture of several phases. Because of the small size of the grains in the mixture, and the intimate intergrowth of the phases comprising it, it has not been possible to identify the individual components. An electron-microprobe analysis of the mixture (Table 3) shows a substantial Se content, which suggests that one of the phases is a selenide or selenate; the reflectance of the components is higher than would be expected for a selenate, so the former is more likely. The analytical shortfall from 100% may be due to an oxide phase in the mixture. The main effect of the alteration has apparently been a decrease in Se and an increase in Cu.

TABLE 1. COMPOSITION OF UMANGITE AND NAUMANNITE FROM THE COPPER HILLS PROSPECT, WESTERN AUSTRALIA

	Umangite, Cu_3Se_2			Naumannite, Ag_2Se		
Cu wt%	51.9	(1.5)	54.7	0.3	(0.3)	-
Ag	1.9	(1.9)	-	71.2	(0.5)	73.2
Hg	1.4	(0.6)	-	0.1	(0.2)	-
Pt	2.0	(0.3)	-	0.2	(0.3)	-
Pd	0.2	(0.1)	-	-		-
S	2.0	(0.4)	-	-		-
Se	43.7	(1.3)	45.3	28.8	(0.4)	26.8
total	103.1		100.0	100.6		100.0

The standard deviation is shown in parentheses. The third and sixth column of data show the theoretical proportion of constituents. The compositions listed are an average result of ten (umangite) and sixteen (naumannite) spot-analyses. Electron-microprobe wavelength-dispersion analyses. Excitation voltage 20 kV; standards: pyrite (S), HgS (Hg), elements for the remainder. Spectral lines: Cu$K\alpha$, Ag$L\alpha$, Hg$L\alpha$, Pt$L\alpha$, Pd$L\alpha$, S$K\alpha$, Se$K\alpha$. Analyst: G.J. Hitchen.

TABLE 2. COMPOSITION OF CHRISSTANLEYITE AND ITS Cu ANALOGUE

	Chrisstanleyite	$Ag_2Pd_3Se_4$	Cu Analogue	$Cu_2Pd_3Se_4$
Cu wt%	2.05	-	16.83	16.68
Ag	24.07	25.36	0.92	-
Hg	0.36	-	-	-
Pt	0.70	-	-	-
Pd	35.48	37.52	40.09	41.88
Se	38.50	37.12	41.33	41.44
total	101.16	100.0	99.17	100.0

Analyst: J. H. G. Laflamme, CANMET. The second and fourth column of data pertain to the theoretical compositions.

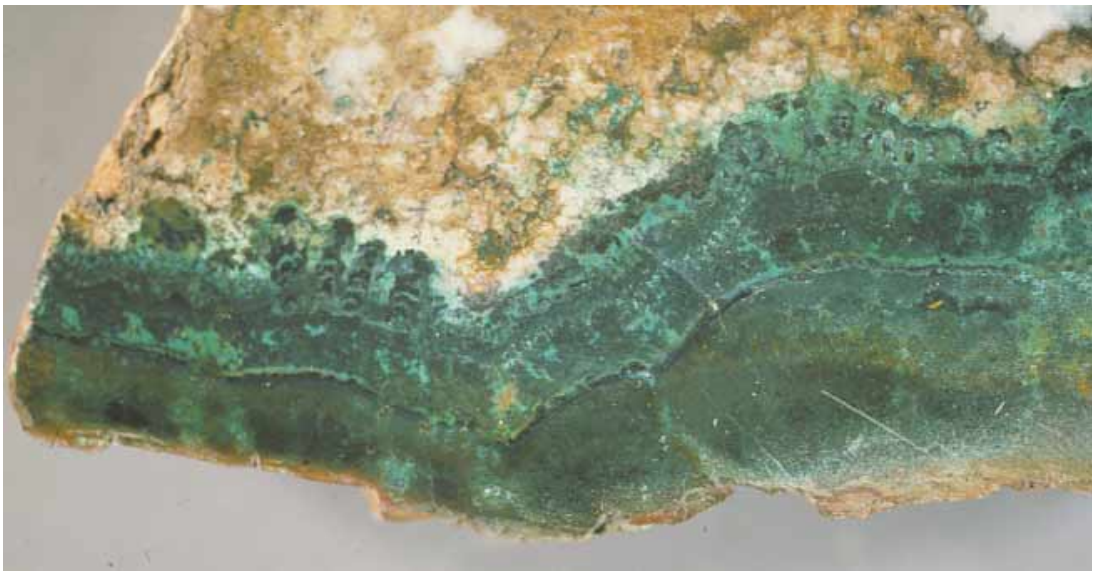

FIG. 1. A polished slab of the vein material illustrating the general nature of the mineralization. The greyish green layer at the bottom is ferruginous malachite; above that is a heterogeneous layer of mineralized (black) and unmineralized malachite (green). Width of field is 80 mm.

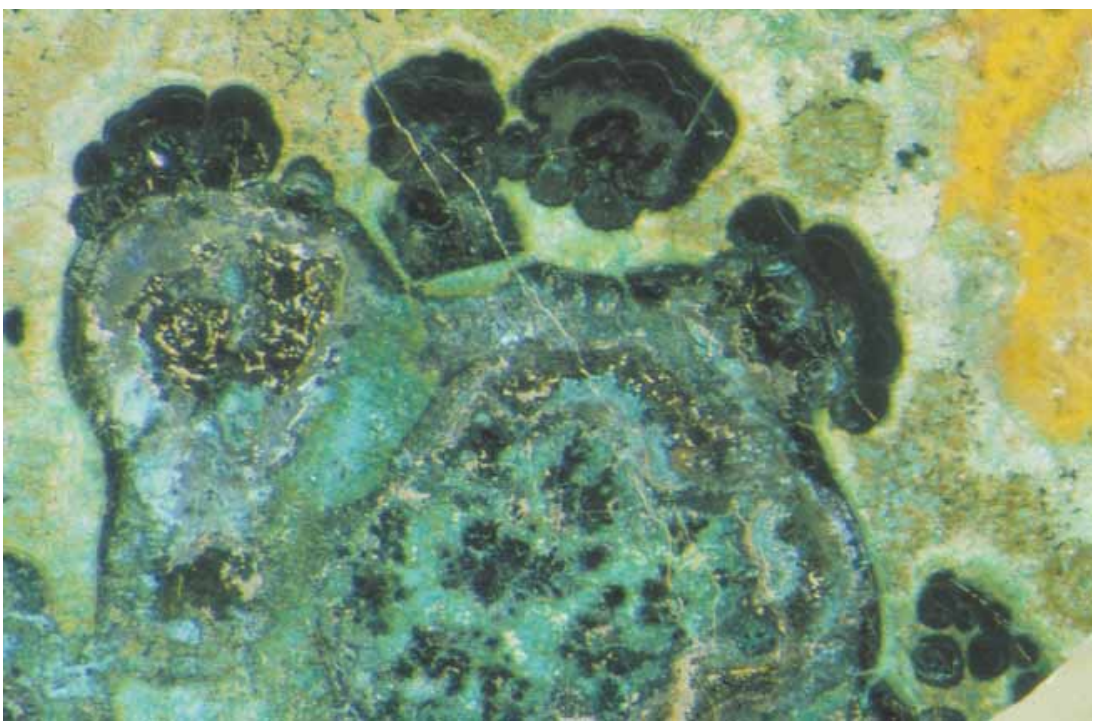

FIG. 2. Photograph of a polished surface in oblique illumination showing a large heterogeneous mass of mineralized malachite (black), unmineralized malachite (green) and quartz (white), with some small grains of chlorargyrite (yellow). The large mass is flanked by a number of dark nodules of mineralized malachite. Width of field is 7 mm.

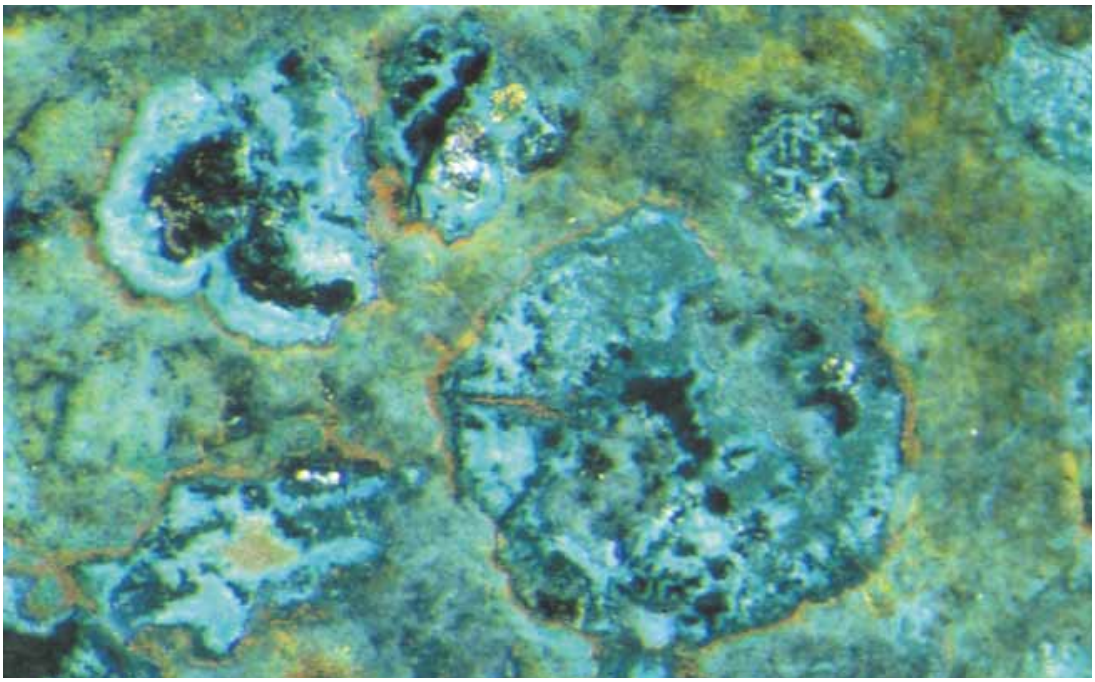

FIG. 3. Photograph of a polished surface in oblique illumination showing several nodules consisting of mineralized malachite (black), unmineralized malachite (green under the microscope but blue in this photo) and quartz (white, grey) in a malachite – quartz – goethite matrix (yellowish green). Width of field is 6 mm.

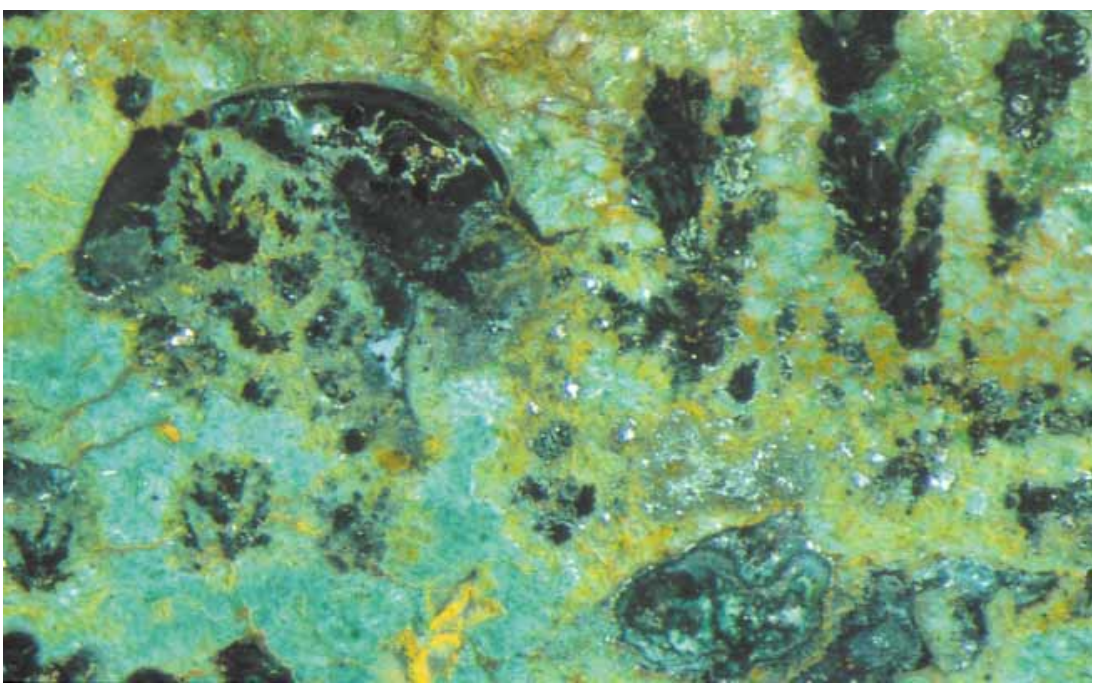

FIG. 4. Photograph of a polished surface in oblique illumination showing a fragment of a spherical nodule and several arborescent fronds of mineralized malachite (black) in a matrix consisting mainly of unmineralized malachite (green under the microscope but blue in this photo) and a quartz – malachite – goethite mixture (yellowish green). Width of field is 11 mm.

Although some of the alteration of the oosterboschite contains remnants of oosterboschite (Fig. 11), most of it does not, and identification in these cases was based on a comparison of energy-dispersion spectra with those of material that contains remanants of oosterboschite.

The product of oosterboschite alteration exhibits a wide range of textures, including disseminated small particles (Fig. 7), larger irregular grains (Fig. 11), intergranular veinlets (Fig. 12), branching veinlets (Fig. 13), conformable layers in malachite nodules (Fig. 8) and arborescent fronds (Fig. 14).

Luberoite (?), Pt_5Se_4

A Pt–Se mineral occurs in the mineralized malachite and, to a lesser degree, in quartz as diffuse "clouds" of dispersed particles, commonly as arborescent forms (Fig. 9), but also as concentrically zoned concentrations (Fig. 8). Electron-microprobe data on such clouds are dominated by Cu, which is interpreted as being due to the malachite host. On the assumption that all the Cu is due to malachite, the composition shown in Table 4 has been augmented by the amounts of CO_2 and H_2O required for the malachite composition. Disregarding the small amount of recorded Ag, the remaining elements give a (Pt,Pd):Se ratio of 5:4, which corresponds to that of luberoite, Pt_5Se_4, a rare mineral heretofore reported from only one occurrence, a placer deposit, and reported to have granodioritic affiliations (Jedwab *et al.* 1992). Unfortunately, the luberoite diagnosis could not be confirmed by X-ray diffraction, as diffraction patterns of the Pt–Se "clouds" showed only malachite.

Native silver and chlorargyrite, AgCl

Native silver occurs in the form of veinlets and irregular masses, in some cases large enough to be visible to the naked eye. The silver shows evidence of partial replacement by chlorargyrite, which emphasizes some of the internal textures, such as the cellular structure shown in Figure 15.

The chlorargyrite contains appreciable bromine, and can therefore be termed a bromian chlorargyrite. Its main occurrence is in the form of nodules (Fig. 16), commonly rimmed by mineralized malachite. A substantial amount of chlorargyrite also occurs as veinlets, which cut all the other minerals in the assemblage, indicating that it is a late mineral in the paragenetic sequence. Some of the chlorargyrite is clearly a replacement of native silver, but some, such as the nodules shown in Figure 16, exhibit no evidence of a silver precursor.

Gold

Gold is abundant in the both the mineralized and ferruginous types of malachite. In the ferruginous malachite, it occurs mainly as disseminated particles, the largest of which are visible to the naked eye. In some mineralized nodules of malachite, the gold occurs as individual particles (Fig. 5), rather like the occurrence of palladium minerals in the same nodules. In others, it occurs as ramifying veinlets (Fig. 17), again like some of the forms exhibited by the palladium minerals. In places, it is closely associated with the silver mineralization, commonly as veinlets and fine-grained dispersions in the chlorargyrite (Fig. 18).

Potarite, PdHg

An essentially isotropic mineral with a high reflectivity and an energy-dispersion spectrum showing only Pd and Hg was provisionally identified as the rare mineral potarite, although the small grain-size and dispersed nature of the mineral precluded positive identification by X-ray diffraction. In a review of the literature on the occurrence of this mineral, Arai *et al.* (1999) concluded that all the descriptions state or imply a secondary hydrothermal origin. At Copper Hills, potarite was seen as tiny grains disseminated in coarse dolomite, several millimeters from the mineralized malachite. Potarite may also be a component in the Pd–Pt oxide mixtures, described below.

TABLE 3. COMPOSITION OF OOSTERBOSCHITE AND OF THE PRODUCT OF ITS ALTERATION

	Oosterboschite, $Pd_4Cu_3Se_5$			Alteration Product	
Pd wt%	43.4	(0.3)	42.1	45.6	(2.0)
Pt	0.4	(0.02)	-	0.3	(0.3)
Hg	-		-	2.4	(1.0)
Cu	17.5	(0.7)	18.9	20.6	(2.7)
Se	45.0	(0.05)	39.0	23.1	(3.4)
total	106.3		100.0	92.0	

The standard deviation is shown in parentheses. The third column of data shows the theoretical proportion of constituents. The compositions listed are an average result of two (oosterboschite) and twenty-two (alteration product) spot-analyses. Electron-microprobe wavelength-dispersion analyses. The conditions are as shown in Table 1. Analyst: G.J. Hitchen.

TABLE 4. COMPOSITION OF Pt–Se "CLOUD"

PtO wt%	21.4	Pt	19.81	0.99
PdO	2.6	Pd	2.3	0.21
AgO	0.6	Ag	0.5	0.04
SeO	9.8	Se	8.1	1.00
CuO*	49.6			
CO_2*	13.7			
H_2O*	5.6			
total	103.3			

* Calculated as components of malachite. Electron-microprobe wavelength-dispersion analyses; operating conditions as in Table 1. Analyst: G. J. Hitchen

FIG. 5. Photomicrograph of polished section in vertical illumination showing a nodule of mineralized malachite containing grains of Pd oxides (grey under the microscope but pale yellow in this photo) and gold (bright yellow); the darker high-relief grains are quartz. Width of field is 2.2 mm.

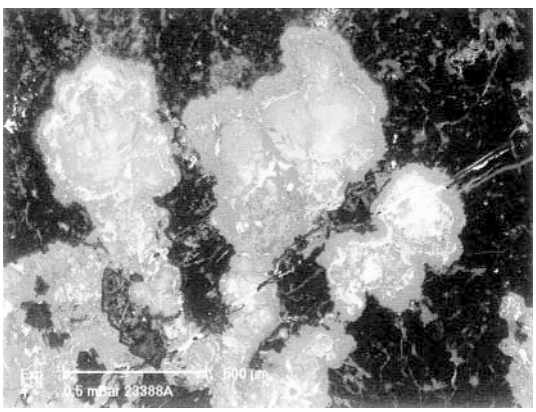

FIG. 6. SEM back-scattered-electron image showing balloon-like formations of mineralized malachite (grey) in quartz (black). The larger white inclusions represent chlorargyrite, and the smaller ones represent the product of alteration of oosterboschite. The cloudy grey areas represent fine-grained dispersions of luberoite (?).

Tiemannite, HgSe

Tiemannite was identified on the basis of its energy-dispersion spectrum and its optical properties; it is isotropic and grey in reflected light. It occurs as small irregular grains, up to about 10 μm in diameter, in the mineralized malachite and as a rim around some grains of naumannite.

Chalcomenite, $CuSeO_3 \cdot 2H_2O$

Chalcomenite occurs as alteration rims around naumannite and chrisstanleyite (Fig. 10), and may also be an alteration product of other selenides as well. It was not possible to obtain a reliable electron-microprobe analysis of the chalcomenite because it decomposes under the electron beam; its identity, however, was confirmed by X-ray-diffraction analysis. In reflected light, it has a low reflectance (similar to that of quartz), and is weakly anisotropic.

Unidentified Pd and Pt oxides

Oxides of palladium and platinum occur in the mineralized malachite mainly as spherical or subspherical grains, commonly arranged in a pattern that conforms to the shape of the nodules (Fig. 5).

Microscopic examination of these grains at high magnification shows that they are an intimate mixture of several phases, the individual components of which could not be identified optically because of their fine-grained nature. They are optically isotropic, with a reflectance similar to that of tetrahedrite (~30%). X-ray powder-diffraction patterns of grains from two specimens (Table 5) exhibit a relatively strong reflection in the region of 2.34 Å, which is the strongest reflection in

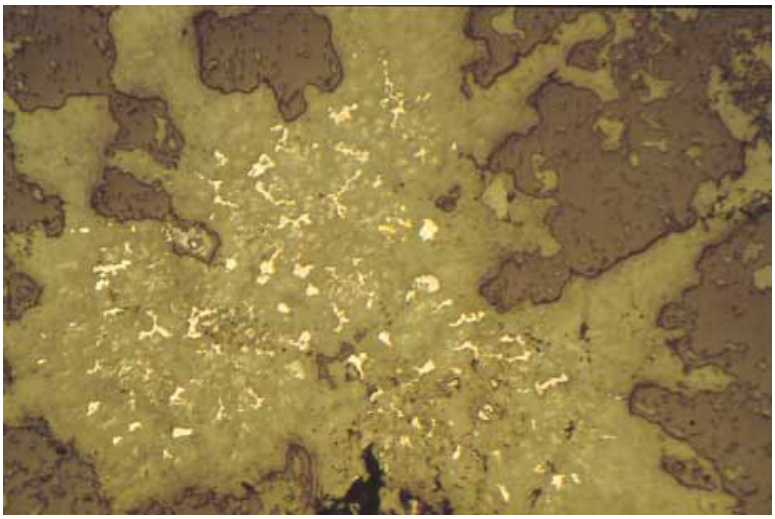

FIG. 7. Photomicrograph of polished section in vertical illumination, showing an irregular grain of mineralized malachite with abundant inclusions of Pd oxides (white) and a few inclusions of gold (yellow); the faint grey mottling is due to clouds of dispersed luberoite (?). Width of field is 1.1 mm.

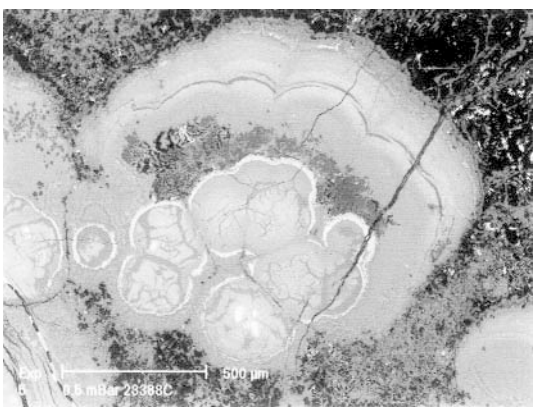

FIG. 8. SEM back-scattered-electron image of one of the black nodules in Figure 2. Concentric layers in shades of grey represent varying concentrations of finely dispersed luberoite (?) in malachite. Pd oxides comprise the thin white layers. Quartz is dark grey.

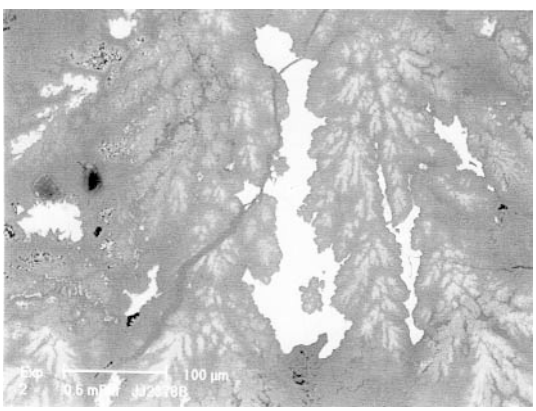

FIG. 9. SEM back-scattered-electron image of one of the arborescent fronds in Figure 4. Large grains of oosterboschite and its alteration product (white) are flanked by arborescent "clouds" of finely dispersed luberoite (?) (in shades of light grey).

the diffraction pattern of potarite. Some of the other weak reflections can be attributed to malachite and quartz (indicated in Table 5). However, this leaves the other reflections, including a strong reflection at 2.552 Å in one of the patterns, unaccounted for. Electron-microprobe analyses (Table 6) demonstrate the great compositional variability of this material. The relatively high Hg contents indicated in two of the analyses (B and D) tend to confirm the presence of potarite.

Unidentified Pt–Cu hydroxide mineral

An unusual Pt–Cu mineral in the assemblage occurs as tiny transparent anisotropic crystals (Fig. 19) within some of the quartz in the nodules of mineralized malachite. An electron-microprobe analysis of these crystals gave a composition corresponding to $Pt_{0.42}Cu_{0.56}Pd_{0.01}Hg_{0.01}Se_{0.10}O_{2.06}$ on the basis of a cation total of 1.00. However, the crystals decomposed under the electron

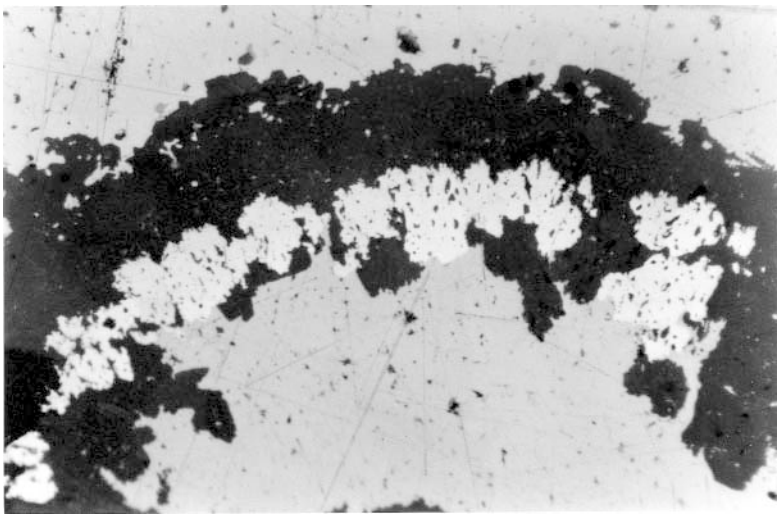

FIG. 10. Photomicrograph of polished section showing naumannite (grey) and the intergrowth of chrisstanleyite and its Cu-dominant analogue (white), separated by chalcomenite (black). Width of field is 1.1 mm.

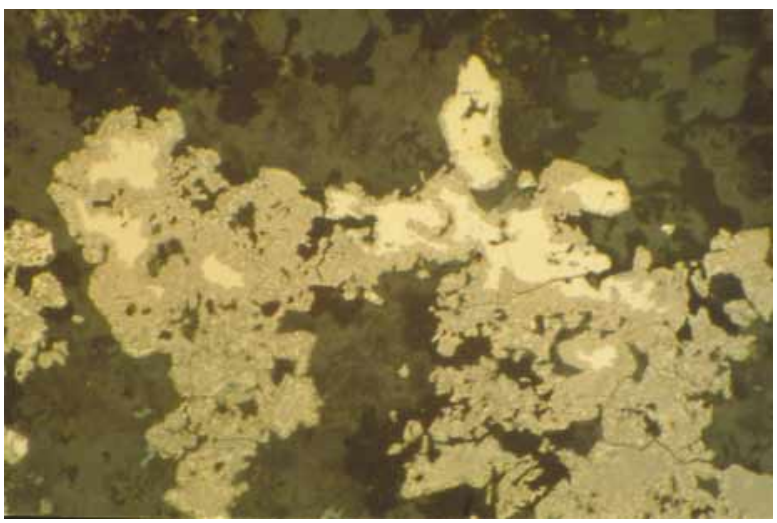

FIG. 11. Photomicrograph of polished section in vertical illumination, showing oosterboschite remnants (yellow) in its alteration product (pale brown). Width of field is 0.2 mm.

beam, and there was an analytical shortfall of 9.6%, suggesting the presence of an unanalyzed volatile component. Carbon was sought, but not detected. Possibly it is a hydroxide, with an idealized composition approximating $(Cu,Pt)(OH)_2$. A mineral of this composition has not been reported in the mineralogical literature. The crystals were found to be too small for characterization by optical or by X-ray-diffraction methods. In polished section, the mineral has a reflectance similar to that of malachite (~10%) and is moderately anisotropic.

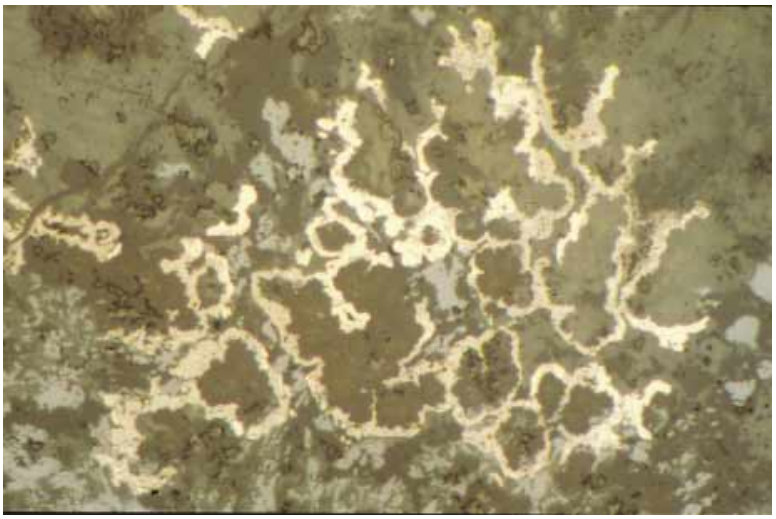

FIG. 12. Photomicrograph of polished section in vertical illumination, showing oosterboschite (yellow) and its alteration product (light brown) as intergranular veinlets surrounding mineralized malachite and quartz (dark grey), and several grains of goethite (light grey). Width of field in 0.56 mm.

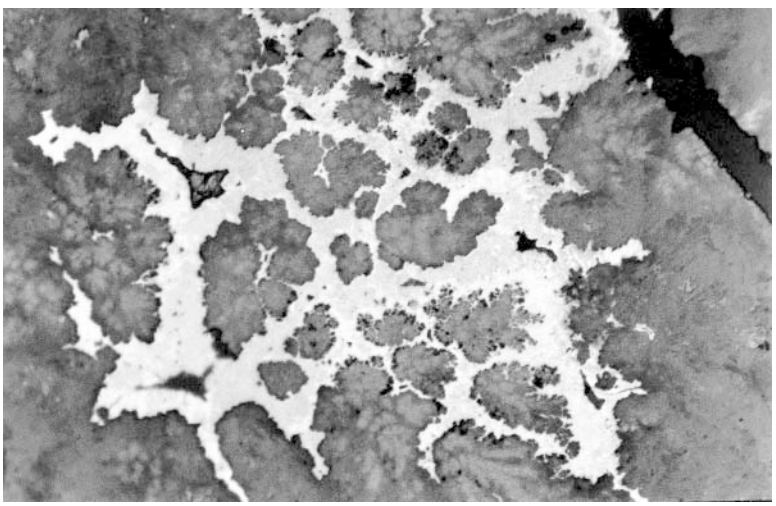

FIG. 13. Photomicrograph of polished section in vertical illumination, showing branching veinlets of the alteration product of oosterboschite (white) enclosing mineralized malachite with clouds of dispersed luberoite (?) (grey). Width of field is 0.56 mm.

Unidentified Pd–Hg–Cu selenide

This mineral occurs as tiny yellow anisotropic crystals, prismatic in section, closely associated with umangite in the ferruginous malachite. Electron-microprobe analyses (Table 7) show that its composition corresponds to $(Pd,Cu,Hg)_{1.16}Se$, with additional minor amounts of Pt and Ag. The generalized formula corresponds reasonably well to that of palladseite, $Pd_{17}Se_{15}$ (Davis *et al.* 1977), except for the major amounts of Hg and Cu present in the mineral. However, palladseite is isotropic, whereas this mineral is highly anisotropic. It

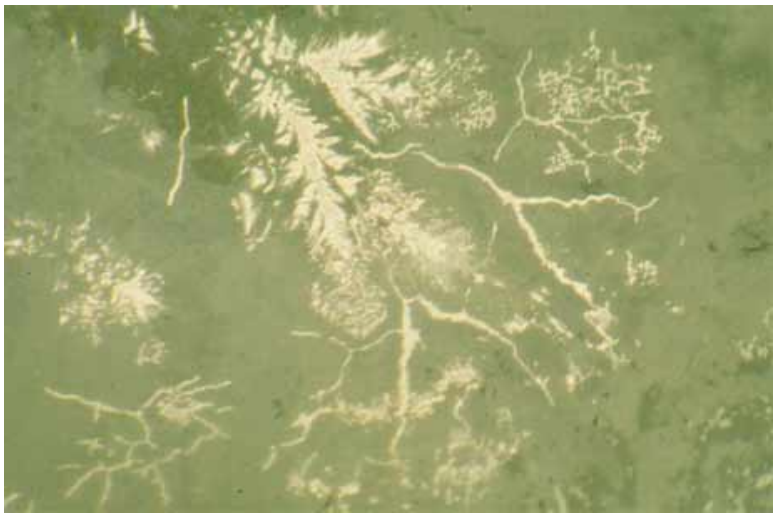

FIG. 14. Photomicrograph of a polished section in vertical illumination, showing veinlets and fern-like fronds of the alteration product of oosterboschite (white) in a matrix of malachite (light grey) and quartz (dark grey). Width of field is 0.2 mm.

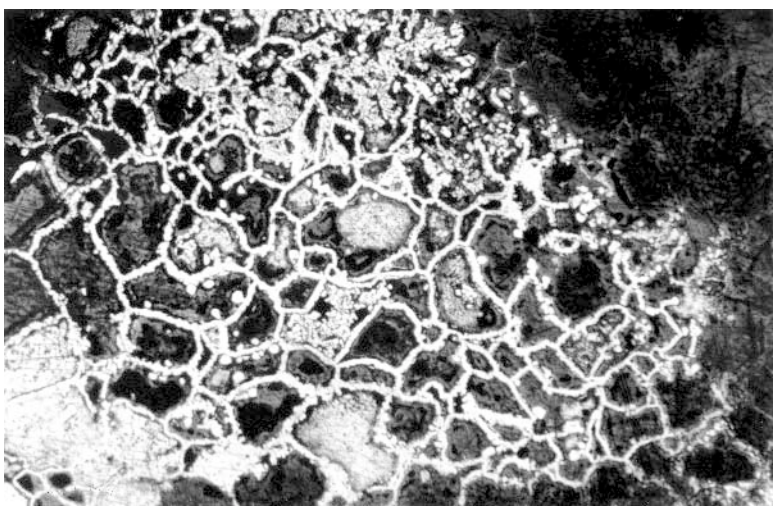

FIG. 15. Photomicrograph of a polished section in vertical illumination, showing native silver (white) with a cellular texture. Most of the cells are filled by chlorargyrite (grey). Width of field is 2.2 mm.

therefore appears to be a new mineral. It could not be fully characterized because of its small grain-size.

DISCUSSION

The mineral assemblage in this occurrence has an unusual bulk composition, with selenium dominant and sulfur virtually absent in the primary minerals. The co-existence of four precious metals, palladium, platinum, gold and silver, in one mineral assemblage is also uncommon.

An ore deposit with some similarities to the Copper Hill occurrence is the Coronation Hill deposit in the Northern Territory of Australia. It contains several types

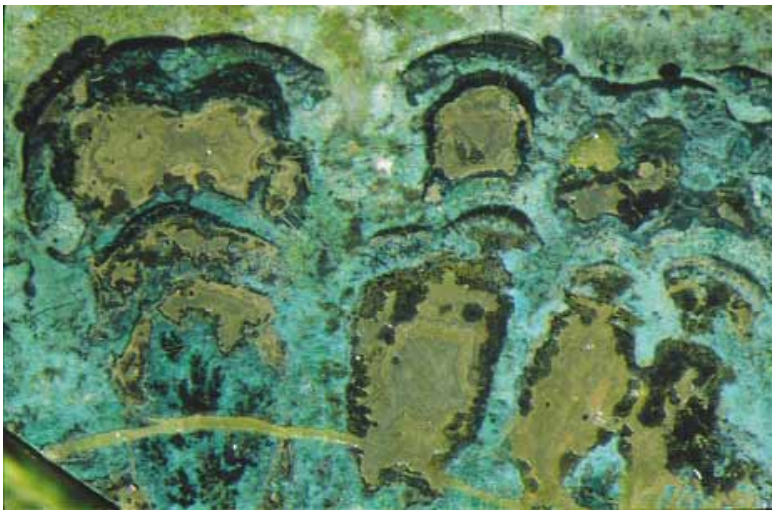

FIG. 16. Photograph of a polished surface in oblique illumination, showing nodules of chlorargyrite (brown) in malachite (green under the microscope but blue in this photo). The dark rims around the chlorargyrite represent mineralized malachite. Width of field is 12 mm.

TABLE 5. X-RAY POWDER-DIFFRACTION DATA FOR TWO Pd–Pt OXIDE MIXTURES

I est.	*d* (Å)	I est.	*d* (Å)	I est.	*d* (Å)	I est.	*d* (Å)
1	6.01*			5	2.334	10	2.345
1	5.09*			1	2.137	2	2.142
2	3.67*			1	2.058		
		2	3.34**	1	1.689		
2	2.870			2	1.620		
10B	2.552	1B	2.552	3	1.271	3	1.274

* Reflections probably due to malachite; ** reflection probably due to quartz.

TABLE 6. COMPOSITION OF Pd–Pt OXIDE MIXTURES

	A	B	C	D
PdO wt%	30.4	62.1	34.6	36.4
PtO	20.0	1.4	-	5.7
HgO	5.9	26.1	9.8	47.1
CuO	43.9	7.7	51.0	14.8
SeO_2	3.4	-	-	-
total	103.6	97.3	95.4	104.0

Electron-microprobe wavelength-dispersion analyses. The conditions are as shown in Table 1. Analyst: G.J. Hitchen.

TABLE 7. COMPOSITION OF UNIDENTIFIED Pd–Hg–Cu SELENIDE

	1	2		1	2
Cu	10.3	0.34	Pd	23.8	0.47
Ag	2.7	0.05	Pt	3.0	0.03
Hg	25.5	0.27	Se	37.6	1.00

Electron-microprobe wavelength-dispersion analyses; operating conditions as in Table 1. Analyst: G. J. Hitchen. Column 1: composition expressed in weight %. Column 2: composition expressed in atomic proportions based on 1.00 atoms of Se.

of mineralization, including a gold – platinum-group element (PGE) – selenide assemblage (Carville *et al.* 1990). The results of microthermometry and low-temperature laser Raman spectroscopy performed on minerals in this assemblage led Mernagh *et al.* (1994) to conclude that the minerals were deposited from a hydrothermal solution of high salinity and low pH at a temperature of about 140°C. Precipitation of the ore minerals was attributed to the interaction of the hydrothermal fluids with feldspathic rocks. Macdonald (1987) regarded the Coronation Hill deposit as a late diagenetic or epithermal type. According to Mountain & Wood (1987), platinum and palladium are soluble in saline fluids at a level of 10 ppb or greater, at low pH and high fugacity of oxygen. Confirmation that contemporary hydrothermal systems can carry appreciable amounts of Au, Ag and PGE has been provided by the chemical analysis of fluid inclusions in sulfide minerals collected from black smoker sulfide deposits in ocean basins (Lysitsyn *et al.* 1999).

It seems, therefore, that a low-temperature hydrothermal origin can be invoked for the Copper Hills oc-

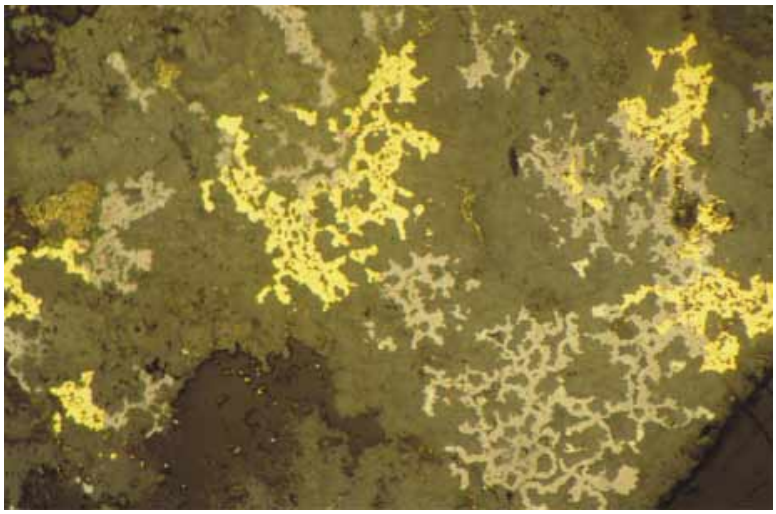

FIG. 17. Photomicrograph of a polished section in vertical illumination, showing ramifying veinlets of gold (yellow) and of the alteration product of oosterboschite (medium grey) in malachite (dark grey). Width of field is 1.1 mm.

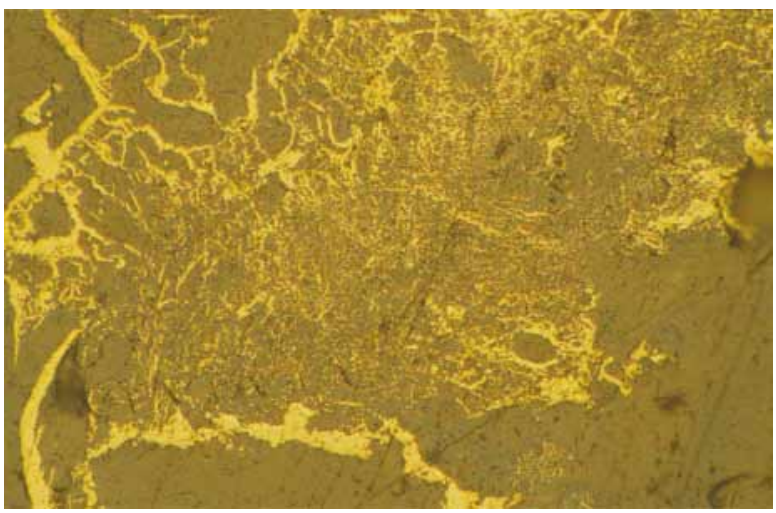

FIG. 18. Photomicrograph of a polished section in vertical illumination, showing gold (yellow) as veinlets and fine-grained dispersions in chlorargyrite (grey). Width of field is 0.2 mm.

currence. In spite of some similarities with the Coronation Hill deposit, the Copper Hills mineralization is unique because of its malachite host. The textural features observed in the intimate association of malachite with the platinum, palladium, gold, silver and mercury minerals provides strong evidence for their cogenesis. Malachite is generally regarded as a secondary copper mineral, but in the botryoidal malachite there is no indication of a copper-bearing precursor, and therefore the malachite is presumed to be a primary product of the hydrothermal mineralization process (although there is finely disseminated berzelianite and umangite in the

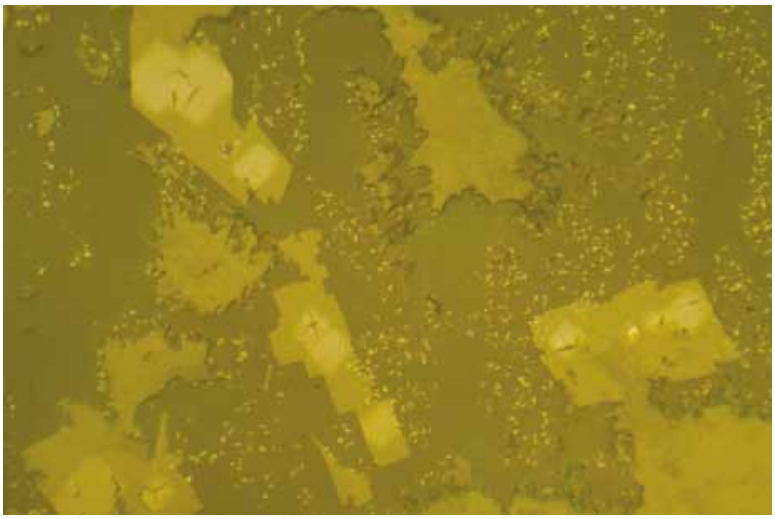

FIG. 19. Photomicrograph of a polished section in vertical illumination, showing crystals of $(Pd,Cu)(OH)_2$ (light grey) in quartz (medium grey). The brighter areas on the crystals indicate damage by the electron beam during electron-microprobe analysis. Width of field is 0.2 mm.

ferruginous malachite, there is no evidence for them being precursors of the botryoidal malachite). A possible explanation for the origin of this assemblage is that acidic hydrothermal solutions containing Cu, Pd, Pt, Au, Ag, Hg and Se reacted with the carbonate unit, resulting in the precipitation of malachite and coprecipitation of the selenides of the various metals. To my knowledge, this is the first reported occurrence of malachite of probable hydrothermal origin.

Although the stability of malachite at room temperature has been well established (*e.g.*, Symes & Kester 1984), less is known about its thermal stability. Thermogravimetric experiments have shown that very finely divided malachite decomposes at 240°C (Simpson *et al.* 1964), so it would seem that its thermal stability is consistent with the temperature regime proposed for the Coronation Hill deposit.

The oxides of palladium and platinum are clearly products of decomposition of the primary selenides, but it is unclear whether this decomposition occurred during emplacement of the mineral assemblage or as the result of later supergene alteration. The literature on PGE oxide minerals is rather sparse, but the following observations can be made. Several mechanisms have been suggested for the origin of PGE oxides found in the Pirogues ophiolite (Augé & Legendre 1994), namely oxidation of PGE alloys, and direct crystallization of the oxides during lateritization). The Pd–Cu oxide reported from an iron mine in the Itabira District of Brazil (Olivo & Gauthier 1995) is believed to have been formed during the hydrothermal mineralization event rather than as a result of weathering processes. Jedwab (1995) favored a supergene origin for this class of minerals.

The mode of occurrence of the Cu–Pt hydroxide mineral found in the Copper Hills assemblage is different from that of the Pd–Pt oxides. It occurs as euhedral crystals entirely enclosed in quartz, and must surely have been precipitated during the hydrothermal crystallization process.

ACKNOWLEDGEMENTS

It gives me great pleasure to dedicate this contribution to Louis Cabri, with whom I had the privilege of working at CANMET for a number of years. I am grateful to the principals of Australian Platinum Mines NL for giving me access to their material, and for permission to publish the results. I also appreciate the assistance rendered by G.J. Hitchen of CSIRO and J.H.G. Laflamme of CANMET, who performed the electron microprobe analyses, and by M.R. Verall of CSIRO, who produced the scanning-electron photographs. I also appreciate helpful comments by the referees, L.J. Cabri and J. Jedwab.

REFERENCES

ARAI, S., PRICHARD, H.M., MATSUMOTO, I. & FISHER, P.C. (1999): Potarite (Pd–Hg) in thermally metamorphosed dunite from the Inazumi-yama ultramafic complex, southwestern Japan: an implication for the behaviour of mercury in PGE mineralization in peridotite. *Mineral. Mag.* **63**, 369-377.

AUGÉ, T. & LEGENDRE, O. (1994): Platinum-group element oxides from the Pirogues ophiolitic mineralization, New Caledonia: origin and significance. *Econ. Geol.* **89**, 1454-1468.

BAGAS, L. (1999): Geology of the Blanche–Cronin 1:100 000 sheet (part sheets 3551 and 3552). *Western Australia Geol. Surv., 1:100 000 Geological Series Explanatory Notes*.

CARVILLE, D.P., LECKIE, J.F., MOORHEAD, C.F., RAYNER, J.G. & DURBIN, A.A. (1990): Coronation Hill gold–platinum–palladium deposit. *In* Geology of the Mineral Deposits of Australia and Papua New Guinea (F.E. Hughes, ed.). *Austral. Inst. Mining Metall., Monogr. Ser.* **14**, 759-762.

DAVIS, R.J., CLARK, A.M. & CRIDDLE, A.J. (1977): Palladseite, a new mineral from Itabira, Minas Gerais, Brazil. *Mineral. Mag.* **41**, 123, M10-M13.

HICKMAN, A.H. & BAGAS, L. (1995): Tectonic evolution and economic geology of the Paterson Orogen – a major reinterpretation based on detailed geological mapping. *Geol. Surv. Western Aust., Annual Review 1993–94*, 67-76.

JEDWAB, J. (1995): Oxygenated platinum-group-element and transition-metal (Ti, Cr, Mn, Fe, Co, Ni) compounds in the supergene domain. *Chronique de la Recherche Minière* **520**, 47-53.

_____, CERVELLE, B., GOUET, G., HUBAUT, X. & PIRET, P. (1992): The new platinum selenide luberoite Pt_5Se_4 from the Lubero region (Kivu Province, Zaire). *Eur. J. Mineral.* **4**, 683-692.

JOHAN, Z., PICOT, P., PIERROT, R. & VERBEEK, T. (1970): L'oosterboschite, $(Pd,Cu)_7Se_5$, une nouvelle espèce minérale, et la trogtalite cupro-palladifère de Musonoï (Katanga). *Bull. Soc. fr. Minéral. Cristallogr.* **93**, 476-481.

LYSITSYN, A.P., LAPUKHOV, A.S., SIMONOV, V.A., SIDENKO, N.V., MAZUROV, M.P., BOGDANOV, YU.A. & BATUEV, V.N. (1999): Noble metals in ore-forming hydrothermal systems of modern oceans. *Dokl. Earth Sci.* **369**, 1198-1200.

MACDONALD, J.A. (1987): Ore deposit model. 12. The platinum group element deposits: classification and genesis. *Geosci. Can.* **14**, 155-166.

MERNAGH, T.P., HEINRICH, C.A., LECKIE, J.F., CARVILLE, D.P., GILBERT, D.J., VALENTA, R.K. & WYBORN, L.A.I. (1994): Chemistry of low-temperature hydrothermal gold, platinum and palladium (± uranium) mineralization at Coronation Hill, Northern Territory, Australia. *Econ. Geol.* **89**, 1053-1073.

MOUNTAIN, B.W. & WOOD, S.A. (1987): Solubility and transport of platinum-group elements in hydrothermal solutions: thermodynamic and physical chemical constraints. *In* GeoPlatinum '87 (H.M. Prichard, P.J. Potts, J.F.W. Bowles & S.J. Cribb, eds.). Elsevier, Amsterdam, The Netherlands (57-82).

NICKEL, E.H. (1998): A remarkable occurrence of Pd–Pt–Au–Ag–Cu–Se mineralisation in Western Australia. *Int. Mineral. Assoc., 17th Gen. Meeting* (*Toronto*), *Abstr.* A-120.

OLIVO, G.R. & GAUTHIER, M. (1995): Palladium minerals from the Cauê iron mine, Itabira District, Minas Gerais, Brazil. *Mineral. Mag.* **59**, 455-463.

PAAR, W.H., ROBERTS, A.C., CRIDDLE, A.J. & TOPA, D. (1998): A new mineral, chrisstanleyite, $Ag_2Pd_3Se_4$, from Hope's Nose, Torquay, Devon, England. *Mineral. Mag.* **62**, 257-264.

SIMPSON, D.R., FISHER, R. & LIBSCH, K. (1964): Thermal stability of azurite and malachite. *Am. Mineral.* **49**, 1111-1114.

SYMES, J.L. & KESTER, D.R. (1984): Thermodynamic stability studies of the basic copper carbonate mineral, malachite. *Geochim. Cosmochim. Acta* **48**, 2219-2229.

Received March 3, 2000, revised manuscript accepted June 30, 2000.